Optimal Thrust Allocation Strategy of Electric Propulsion Ship Based on Improved Non-Dominated Sorting Genetic Algorithm II

Diju Gao, Xuyang Wang, Tianzhen Wang, Yide Wang, Xiaobin Xu

IEEE Access
Multidisciplinary | Rapid Review | Open Access Journal

Received August 23, 2019, accepted September 16, 2019, date of publication September 18, 2019,
date of current version September 30, 2019.

Digital Object Identifier 10.1109/ACCESS.2019.2942170

Optimal Thrust Allocation Strategy of Electric Propulsion Ship Based on Improved Non-Dominated Sorting Genetic Algorithm II

DIJU GAO[1], XUYANG WANG[1], TIANZHEN WANG[1], YIDE WANG[1,2], AND XIAOBIN XU[3]
[1]Key Laboratory of Marine Technology and Control Engineering, Ministry of Transport, Shanghai Maritime University, Shanghai 201306, China
[2]Institut d'Electronique et de Télécommunications de Rennes, UMR CNRS 6164, Universite de Nantes, 44300 Nantes, France
[3]School of Automation, Hangzhou Dianzi University, Hangzhou 100084, China

Corresponding author: Xuyang Wang (wxyautomation@163.com)

This work was supported in part by the National Natural Science Foundation of China under Grant 61673260 and Grant 61304186, and in part by the NSFC-Zhejiang Joint Fund for the Integration of Industrialization and Informatization under Grant U1709215.

ABSTRACT The azimuth thruster is widely used in electric propulsion ships due to its excellent performance. The thrust allocation (TA) method of multi-azimuth thruster is the key technology in ship motion control. The purpose of TA is to accurately distribute the thrust and angle of each thruster to provide the vessel the required force and moment. A TA strategy based on the improved non-dominated sorting genetic algorithm II (INSGA-II) is developed in this study. The algorithm introduces the differential mutation operator in the differential evolution (DE) to replace the polynomial variation in NSGA-II, which improves the local optimization ability of the algorithm. The effectiveness of the TA strategy based on INSGA-II algorithm is illustrated by simulations.

INDEX TERMS Electric propulsion, multi-azimuth thruster, thrust allocation, optimization, NSGA-II.

I. INTRODUCTION

Due to the breakthrough in efficiency, maneuverability, reliability and flexibility of operations, the application of electric propulsion is widespread [1]. The azimuth thruster can make a 360-degree revolution around the axis and achieve maximum thrust in any direction. It can make the ship rotate, move laterally, and retreat in a special driving operation. Azimuth thrusters are installed on various engineering vessels, such as tugboats, floating crane vessels, dredgers, ferries, and working pontoons [2], [3]. In order to improve the maneuverability, efficiency and system dependability of engineering vessels, more than two propellers are usually deployed. For example, tugs are equipped with multiple propellers at the stern, midship and bow [4]. However, on the one hand, the interaction of the propellers causes asymmetric and irregular dynamic turbulence characteristics in the propeller propulsion operation, which poses a challenge to the control of the ship. On the other hand, the propulsion load fluctuates drastically under complex sea environment, making the power distribution of each propeller unbalanced. Therefore, the accurate allocation of each azimuth thruster is a key issue to enable the electric propulsion ship to obtain the required force and moment.

In complex sea conditions, the ship usually has six degrees of freedom (DOFs) due to the action of wind, current and waves. The movements can be decomposed into two parts: high frequency and low frequency motions. The high-frequency part is caused by the reciprocation and undulation of the wave. Active control of the high-frequency part may lead to repeated fluctuations in the control output, propeller wear, and grid variations. Therefore, the high-frequency component is generally removed by filtering, such that only three DOFs motions of ship are studied (surge, sway and yaw) [5]. For an electric propulsion ship equipped with azimuth thrusters, the system is an over-actuated system. The function of the thrust allocation (TA) is to use redundant propellers to select the optimal solution from propellers satisfying the control mapping relationship to improve the fault tolerance and maneuverability while reducing the power consumption. Therefore, the TA problem of the azimuth thrusters is essentially a constrained nonlinear multi-objective optimization problem.

The associate editor coordinating the review of this manuscript and approving it for publication was Juntao Fei.

When the thruster direction is fixed or the thruster and rudder are fixed on a plane to provide the required thrust, the TA problem can be approximated as an unconstrained least squares problem. The problem can be solved by the explicit Moore-Penrose solutions [5], [6]. By introducing the mechanical constraints of the thruster, the constrained TA optimization problem can be solved by an iterative solution. Johansen proposed a quadratic programming (QP) based method to solve such problem [7]. For ships equipped with multiple azimuth thrusters, the thrust structure is complex and the feasible field of the variable is large. Liang proposed a method using the sequential quadratic programming (SQP) to solve the non-convex nonlinear optimization problem [8]. The real-time performance and local optimization capabilities of QP and SQP are excellent, while the ability to find the global optimal solution in a wide range is relatively poor. Therefore, the TA method based on the basic intelligent algorithms is proposed in [9], [10]. However, the basic intelligent algorithms have some drawbacks in terms of convergence speed and diversity. Some researchers have developed the improved basic intelligent algorithms [11]–[13]. However, the convergence of the improved intelligent algorithms cannot be guaranteed. Based on the improved intelligent algorithms, Wu proposed the adaptive hybrid artificial bee colony algorithm (AHABCC), which can adaptively switch the search mechanisms based on the number of iterative solutions [14]. However, the search method combining the mutation operator in differential evolution (DE) with the social cognitive function of particle swarm optimization (PSO) is not perfect, and the control parameters need to be tested repeatedly. Hybrid algorithm based on the genetic algorithm (GA) and SQP was proposed by Zhao and Roh [15]. Guo proposed a new algorithm combining the biogeography-based optimization (BBO) and PSO [16]. However, the hybrid intelligent algorithms cannot guarantee the stability.

The main contributions of this paper are as follows:

1) NSGA-II is applied to deal with multi-variables, multi-constraints and non-convex objective function, which solves the optimal thrust allocation problem of electric propulsion ship with multi-azimuth thrusters.
2) The thrust allocation of electric propulsion ship with multi-azimuth thrusters requires not only the control accuracy and maneuverability of the ship, but also the reduction of energy consumption and mechanical wear, which often lead to the suboptimal solution of the propellers state. The improved NSGA-II is introduced, which uses the difference operator in differential evolution algorithm to improve the mutation operation. INSGA-II is applied to the TA, which solves the problem that the state of the propellers is easy to fall into local optimum. The proposed ship thrust allocation algorithm reduces the energy consumption of the thrusters and improves the control precision.
3) By comparing INSGA-II with SQP, the average thrust errors of INSGA-II in 3 DOFs motions of ship (surge, sway and yaw) are 29.7%, 25% and 22.5% of those of SQP, respectively. The maximum power consumption and average power consumption of INSGA-II are 86.1% and 80.4% of those of SQP, respectively. The simulation results verify the effectiveness of the proposed thrust allocation algorithm based on INSGA-II.

The remaining of the paper is organized as follows. Section II presents the mathematical model for multi-objective optimization of thrust allocation problem. Section III presents an improved NSGA-II algorithm and applies it to thrust allocation. In Section IV, the proposed algorithm is applied to the Cybership III by simulations, and the obtained results are analyzed in detail. Section V concludes the paper.

II. THRUST ALLOCATION MATHEMATICAL MODEL

A. PROBLEM OVERVIEW

The TA optimization model is established based on CyberShip III tug model with a micro scale of 1:30 [4], [17], [18]. The layout of the thruster is shown in Fig.1. 1#-3# are all azimuth thrusters and 4# is a tunnel thruster. The tunnel thruster is the side thruster of the ship and its direction cannot be changed. In this paper, subscripts i and j both indicate the number of the propeller ($i = 1, 2, 3; j = 1, 2, 3, 4$).

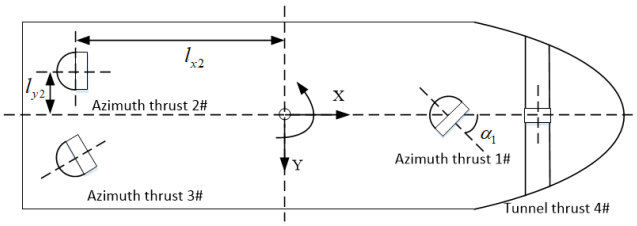

FIGURE 1. Thrust layout of CyberShip III.

Geodetic coordinate system X_EOY_E and the hull coordinate system XOY are used to describe the movement of the ship in three DOFs. Both XY and X_EY_E are coincided with the horizontal plane. The position and yaw angle vector of the ship in the geodetic coordinate system is denoted by $\boldsymbol{\eta} = [x, y, \psi]^T$, and the velocity vector of the three DOFs in the hull coordinate system is $\mathbf{v} = [u, v, r]^T$. The relationship between $\boldsymbol{\eta}$ and $\mathbf{v}$ can be described by [5]

$$\dot{\boldsymbol{\eta}} = \mathbf{R}(\psi)\mathbf{v} \tag{1}$$

where

$$\mathbf{R}(\psi) = \begin{bmatrix} \cos(\psi) & -\sin(\psi) & 0 \\ \sin(\psi) & \cos(\psi) & 0 \\ 0 & 0 & 1 \end{bmatrix} \tag{2}$$

The kinematic equation of the hull can be expressed as:

$$\mathbf{M}\dot{\mathbf{v}} + \mathbf{C}(\mathbf{v})\mathbf{v} + \mathbf{D}(\mathbf{v})\mathbf{v} = \boldsymbol{\tau} \tag{3}$$

where $\mathbf{M}$ is the inertia matrix of the hull; $\mathbf{C}(\mathbf{v})$ represents the Coriolis centripetal force matrix; $\mathbf{D}(\mathbf{v})$ is the damping

matrix [4]; and $\boldsymbol{\tau}$ is the resultant force or torque generated by the driving system, which consists of the working state of the propeller and the thrust structure:

$$\boldsymbol{\tau} = \mathbf{B}(\boldsymbol{\alpha})\mathbf{f} \tag{4}$$

where $\mathbf{f} = [f_1, f_2, f_3, f_4]^T$ is the thrust vector composed of each thruster; $f_1 - f_4$ are the thrusts generated by the 1#-4# thrusters; $\boldsymbol{\alpha} = [\alpha_1, \alpha_2, \alpha_3]^T$. $\alpha_1 \sim \alpha_3$ are the angles of the thruster 1#-3#, respectively. The direction of the tunnel thruster cannot be changed. $\mathbf{B}(\boldsymbol{\alpha}) \in R^{3\times4}$ is the thrust structure matrix representing the mapping relationship from the thrust of each propeller f_i to the resultant force or moment $\boldsymbol{\tau}$. The thrust structure vectors of the azimuth thruster and the tunnel thruster are $\mathbf{b}_a(\alpha_i)$ and $\mathbf{b}_t$, respectively [19], they are given by

$$\begin{aligned} \mathbf{b}_a(\alpha_i) &= \begin{bmatrix} \cos\alpha_i \\ \sin\alpha_i \\ \sin\alpha_i l_{xi} - \cos\alpha_i l_{yi} \end{bmatrix}, \quad \mathbf{b}_t = \begin{bmatrix} 0 \\ 1 \\ l_{x4} \end{bmatrix} \\ \mathbf{B}(\boldsymbol{\alpha}) &= [\mathbf{b}_a(\alpha_1), \mathbf{b}_a(\alpha_2), \mathbf{b}_a(\alpha_3), \mathbf{b}_t] \\ \boldsymbol{\alpha} &= [\alpha_1, \alpha_2, \alpha_3]^T \end{aligned} \tag{5}$$

The controller gives the desired resultant force or moment $\tau_{\mathbf{d}} = [\boldsymbol{\tau}_{\mathbf{x}}, \tau_{\mathbf{y}}, \boldsymbol{\tau}_{\mathbf{z}}]^T$ according to the current ship positions $\eta = [x, y, \psi]^T$,$\mathbf{v} = [u, v, r]^T$. $\boldsymbol{\tau}_{\mathbf{x}}$ and $\boldsymbol{\tau}_{\mathbf{y}}$ are the forces in the X and Y directions, respectively, and $\boldsymbol{\tau}_{\mathbf{z}}$ is the yaw direction torque. The thrust allocation algorithm assigns the respective state quantities α_i and f_j to each thruster according to $\boldsymbol{\tau}_{\mathbf{d}}$, and the resultant force or moment $\boldsymbol{\tau}$ generated by the final thrust system. The block diagram of the ship motion control system is shown in Fig.2.

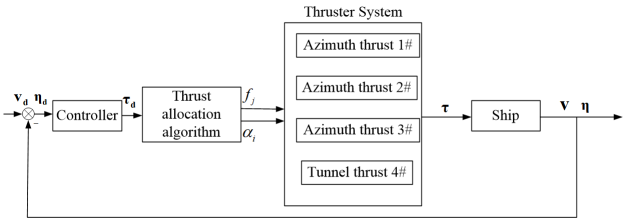

FIGURE 2. Block diagram of the ship motion control system.

B. THRUST ALLOCATION OPTIMIZATION MODEL

Based on the CyberShip III tug model, the forces of the X and Y axes and the total torque can be formulated as follows:

$$\begin{cases} f_x = f_1\cos\alpha_1 + f_2\cos\alpha_2 + f_3\cos\alpha_3 \\ f_y = f_1\sin\alpha_1 + f_2\sin\alpha_2 + f_3\sin\alpha_3 + f_4 \\ m = -f_1\sin\alpha_1 l_{x1} + f_1\cos\alpha_1 l_{y1} + f_2\sin\alpha_2 l_{x2} + f_2\cos\alpha_2 l_{y2} \\ \quad + f_3\sin\alpha_3 l_{x3} - f_3\cos\alpha_3 l_{y3} - f_4 l_{x4} \end{cases} \tag{6}$$

where $\mathbf{l}_j = [l_{xj}, l_{yj}]^T$ is the position vector of the thruster in the hull coordinate system; l_{xj} and l_{yj} are the distances between thruster j# and the X axis and Y axis, respectively.

1) TOTAL POWER CONSUMPTION OF THRUSTERS

For an electric propulsion system, the load on the propulsion unit generally accounts for the largest proportion of the entire power system. The TA of propellers will have a great impact on the entire electrical load, and the repeated fluctuations in the propulsion system power consumption will lead to the collapse of the power system [14]. Minimizing the power of the propulsion system under the premise of satisfying the thrust demand can not only reduce the energy consumption, but also stabilize the output power at a lower level and improve the overall system safety performance. Therefore, the mathematical connection between the thrust generated by the thruster and the corresponding power consumption should be established, and the power consumption should be promoted as a goal to be minimized. The overall power consumption of the thruster can be constructed as [20], [21]:

$$P_w = \sum_{j=1}^{4} c_j \left|f_j\right|^{\frac{3}{2}} \tag{7}$$

where c_j is the power factor of the thruster.

2) THRUST ERROR

The TA algorithm assigns the state quantities α_i and f_j to the corresponding thruster according to $\boldsymbol{\tau}_{\mathbf{d}}$, and the resultant force $\boldsymbol{\tau}$ generated by the propulsion system. The error $\mathbf{s}$ between $\tau_{\mathbf{d}}$ and $\boldsymbol{\tau}$ causes a drop in the control accuracy, resulting in a deviation in the position of the vessel. Therefore, one of the optimization goals of thrust allocation is to minimize the error. The quadratic penalty term J_e for error $\mathbf{s}$ can be defined as

$$\mathbf{s} = \boldsymbol{\tau}_{\mathbf{d}} - \boldsymbol{\tau} \tag{8}$$

$$J_e = \mathbf{s}^{\mathrm{T}}\mathbf{Q}\mathbf{s} \tag{9}$$

where $\mathbf{Q} = diag(\mathrm{w}_x, \mathrm{w}_y, \mathrm{w}_m)$ represents the penalty weight of the resultant force error on the three DOFs [12].

3) MECHANICAL LIMITATIONS OF THRUSTERS

The mechanical limitations of thrusters are mainly reflected in the following aspects: the thrust generated by the full-rotation thrusters at the maximum power when driving ahead and reversing, the change rate of thrust value, the change rate of propeller angle, and the repeated wear limitation of thrusters. Let the maximum output forward thrust and reverse thrust of the propeller be $f_{j\max}$ and $f_{j\min}$, respectively; f_{j0} be the thrust generated by the propeller in the previous step, and f_{jp} be the thrust at the current moment. And let $\alpha_{i\max}$ and $\alpha_{i\min}$ be the upper and lower limits of the propeller rotation angle, respectively; α_{i0} be the angle of the propeller in the previous step, and α_{ip} be the angle of the propeller at the current moment. Due to the mechanical limitations of the thruster, the thruster angle and thrust cannot be transient. Let $f_{j\min}$ and $f_{j\max}$ be the lower and upper limits of the thrust change rate; $\alpha_{i\min}$ and $\alpha_{i\max}$ be the lower and upper limits of the angle change rate of the thrusters, respectively.

The constraints can be expressed as follows:

$$\begin{aligned} f_{j\min} &\le f_{jp} \le f_{j\max} \\ \alpha_{i\min} &\le \alpha_{ip} \le \alpha_{i\max} \\ \Delta f_{j\min} &\le \left|f_{jp} - f_{j0}\right| \le \Delta f_{j\max} \\ \Delta\alpha_{i\min} &\le \left|\alpha_{ip} - \alpha_{i0}\right| \le \Delta\alpha_{i\max} \end{aligned} \tag{10}$$

Let $\boldsymbol{\alpha_p} = [\alpha_{1p}, \alpha_{2p}, \alpha_{3p}]^{\mathrm{T}}$, $\boldsymbol{\alpha_0} = [\alpha_{10}, \alpha_{20}, \alpha_{30}]^{\mathrm{T}}$. In order to avoid the frequent change of the angle of the full-turn propeller, causing the mechanical equipment wear, the following quadratic penalty term J_Ω is introduced for the angle change amount $\Delta\boldsymbol{\alpha} = \boldsymbol{\alpha_p} - \boldsymbol{\alpha_0}$:

$$J_\Omega = (\boldsymbol{\alpha_p} - \boldsymbol{\alpha_0})^T \Omega (\boldsymbol{\alpha_p} - \boldsymbol{\alpha_0}) \tag{11}$$

where $\Omega = diag(\mathrm{w}_1, \mathrm{w}_2, \mathrm{w}_3)$ is the penalty matrix for each angular variation. For example, in the tugboat model studied in this paper, the rotational cost of the full-turn propellers 2#, 3# will be higher, and the corresponding weights in the matrix will be designed to be higher [4].

4) SINGULAR STRUCTURE

In the study of TA, the singular thrust structure means that the current propulsion system cannot produce the resultant force or moment in the freedom of movement of the hull [22]. When approaching a singular structure, the thruster needs to produce a higher thrust output to meet the requirements of working conditions, essentially by reducing the propulsion efficiency in exchange for ship maneuverability. An increase in the thrust output of the propeller can result in more fuel consumption and grid fluctuations, which can even seriously affect the ship operation [23]. Therefore, one of the optimization goals of TA is to prevent the propulsion system from approaching its singular structure.

Therefore, the introduction of a singular structure penalty term J_s allows the TA algorithm to make tradeoffs between the optimal energy consumption and optimal mobility:

$$J_s = \frac{\delta}{\varepsilon + \det(\mathbf{B}(\alpha)\mathbf{B}^{\mathrm{T}}(\boldsymbol{\alpha}))} \tag{12}$$

where $\det(\cdot)$ indicates the matrix determinant operation. In order to avoid numerical problems with a zero denominator, parameter $\varepsilon > 0$ is set to be a very small value. δ is the weight of the singular value penalty term. The bigger the value of δ-c_j is, the more the TA algorithm is focused on the maneuverability.

In summary, the optimization objective function of the TA problem can be expressed as follows:

$$\begin{aligned} \min J(\boldsymbol{\alpha}, f, \mathbf{s}) &= \min\left(P_{\mathrm{w}} + J_e + J_\Omega + J_s\right) \\ &= \min\Big(\sum_{j=1}^{4} c_j \left|f_j\right|^{\frac{3}{2}} + \mathbf{s}^{\mathrm{T}}\mathbf{Q}\mathbf{s} + (\boldsymbol{\alpha_p} - \boldsymbol{\alpha_0})^{\mathrm{T}} \\ &\quad \Omega(\boldsymbol{\alpha_p} - \boldsymbol{\alpha_0}) + \frac{\delta}{\varepsilon + \det(\mathbf{B}(\boldsymbol{\alpha})\mathbf{B}^{\mathrm{T}}(\boldsymbol{\alpha}))}\Big) \end{aligned} \tag{13}$$

$$s.t \begin{cases} f_{j\min} \le f_{jp} \le f_{j\max} \\ \alpha_{i\min} \le \alpha_{ip} \le \alpha_{i\max} \\ \Delta f_{j\min} \le \left|f_{jp} - f_{j0}\right| \le \Delta f_{j\max} \\ \Delta\alpha_{i\min} \le \left|\alpha_{ip} - \alpha_{i0}\right| \le \Delta\alpha_{i\max} \end{cases} \tag{14}$$

III. THRUST ALLOCATION ALGORITHM

Although the traditional NSGA-II algorithm increases the population diversity through the crowding distance mechanism, there are still problems of poor distribution and local optimum [24], [25]. The long-term suboptimal solution of the propellers state will result in a decrease in energy efficiency and mobility. In recent years, many scholars have tried to improve the NSGA-II in terms of the convergence performance and the uniformity of the solution set distribution and apply it to different fields. Therefore, in this paper, we have introduced an INSGA-II and innovatively proposed a thrust distribution algorithm based on INSGA-II [26]. The applied INSGA-II has been improved in the mutation mode, and the differential mutation operator in differential evolution is introduced to improve the global optimization ability of the algorithm.

A. INSGA-II ALGORITHM

NSGA-II is multi-objective optimization algorithm based on genetic algorithm and Pareto optimal solution. The steps of the NSGA-II algorithm are: the initial population of size n is randomly generated firstly. After the non-dominated sorting, the first generation of the offspring population is obtained by some basic operations (selection, crossover, mutation) of the genetic algorithm. Then, the parent population and the offspring population are merged for fast non-dominated sorting. At the same time, the congestion degree is calculated for each individual in the non-dominated layer. The appropriate individuals are chosen according to the non-dominated relationships and individual crowding to form the new parent population. Finally, a new generation of populations is generated by selection, crossover and mutation operators of the genetic algorithm until the ending conditions of the program are met. The flow chart of the NSGA-II algorithm is shown in Fig.3.

It is limited to judge the distribution of individuals only from the size of crowding distance. When there is an error between the current thrust and the desired resultant force, the magnitude and variation range of the thrust error penalty term will be higher than other objective function terms. Solutions that meet the thrust balance conditions will rapidly develop offspring and dominant populations. Therefore, the differential mutation operator is introduced to avoid the premature convergence and local optimum [26], [27].

Specifically, for an initial population P_0, there is a parental entity P_1. The temporary offspring P_2 is generated by mutation operators as follows:

$$P_2 = \beta P_r + (1 - \beta) P_1 \tag{15}$$

where $\beta \in [\sigma_{\min}, 1]$ is a real number that controls the amplification of the difference $(P_r - P_1)$ [28]. A number of

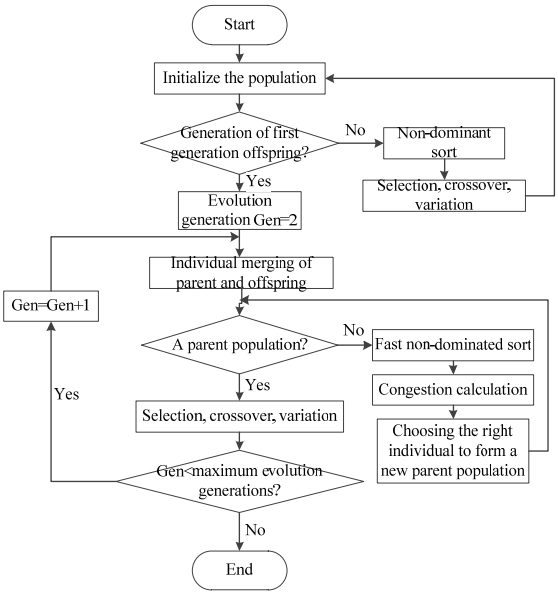

FIGURE 3. Flow chart of the NSGA-II algorithm.

existing studies provide a range of recommended values for β [29], [30]. β can be calculated according to the following scheme :

$$\beta = \begin{cases} \max(\sigma_{\min}, 1 - \left|\dfrac{\beta_{\max}}{\beta_{\min}}\right|), & \text{if } \left|\dfrac{\beta_{\max}}{\beta_{\min}}\right| < 1 \\ \max(\sigma_{\min}, 1 - \left|\dfrac{\beta_{\min}}{\beta_{\max}}\right|), & \text{otherwise} \end{cases} \tag{16}$$

$\beta_{\max}$ and $\beta_{\min}$ are the maximum and minimum values of P_1, respectively. $\sigma_{\min}$ is the lower bound of β. In this paper, $\sigma_{\min} = 0.5$ is used. The function of mutation operator in the early stage of evolution is to maintain the diversity of population. A larger value of β means a greater degree of influence. The operator is not affected by other factors, and can expand the search range to a wider range of search directions. The directional guidance of the difference vector is used to guide the population to search for the optimal solution.

Two important operators are included in the search method here: the threshold value and selection of adjacent individuals. Two extreme endpoints of the non-dominated set $F(k)$ are firstly identified under sub target k. E is the difference between the two extreme values. The threshold value D_k of sub target k is calculated as follows:

$$D_k = \frac{2E}{|F(k)| - 1} \tag{17}$$

where $|F(k)|$ is the number of the elements in $F(k)$. The distance threshold D_k will be dynamically adjusted with the non-dominated set of the contemporary population $F(k)$ [19]. The crowding distance D_k varies with the range of the non-dominant set of the current population. With the process of evolution, the front of non-dominated set is evenly distributed.

In order to prevent the premature convergence, the selection of adjacent individuals is very important. Firstly, sort the non-dominated set $F(k)$ under sub target k; secondly, the distance between the two adjacent individuals is compared with the threshold value D_k. If the individual distance is greater than or equal to D_k, the target values of the adjacent individuals under other sub-objects need to be further computed. If at least one pair of target values is not equal, the pair of adjacent individuals will not meet the requirements of evolution. The adjacent individual pair must perform a differential local search.

B. APPLICATION OF THE INSGA-II

The multi-objective optimization problem (13) of the minimum overall power consumption, minimum thrust error, minimum mechanical wear and maximum maneuverability is firstly established. Then the parameters to be optimized are determined, and the thrust and angle constraints (14) of the propeller are added. Finally, INSGA-II is designed to handle the multi-objective optimization, and the thrust and angle control quantities of each propeller are obtained.

The implementation steps of the algorithm are as follows:

Step1: Establish the optimization model for the minimum overall power consumption, minimum thrust error, minimum mechanical wear, and maximum maneuverability for the TA problem, as shown in (13).

Step2: Select the corresponding constraints of the thrust and angle constraints of the propellers, as shown in (14).

Step3: Use the desired surge, sway resultant force and swaying moment as the input thrust command. Determine the parameters range of the thrust allocation system.

Step4: The INSGA-II is briefly summarized into the following steps:

Step4-1: Select the thrust and angle of the thrusters as the input variables of the algorithm, and design the chromosome as $Ch = \{\alpha_1, \alpha_2, \alpha_3, f_1, f_2, f_3, f_4\}$ according to the configuration of the propellers. The original population P_t with population size n was obtained by initializing the population.

Step4-2: A polynomial mutation is performed on P_t to produce the first generation of offspring Q_t.

Step4-3: Combine populations P_t and Q_t, to get the R_t (a population that temporarily stores population information).

Step4-4: Calculate the objective function value of the individual in the population according to (13). A fast non-dominated sorting of R_t is obtained, and its former i-part composition F_i is obtained.

Step4-5: Calculate the crowding distances for each individual of F_i in the non-dominated layer, and sort the individuals in descending order of crowded distance.

Step4-6: If $F_i + P_t < N$, $P_t = P_t \cup F_i$, $i = i+1$, go back to **Step4-4**; otherwise, return to **Step4-5**. Select the first $N - P_t$ of the F_i into P_t.

Step4-7: If $t \geq G_{\max}$ ($G_{\max}$ is the maximum iteration number), the non-dominant individual in P_t is outputted and the algorithm stops; otherwise, P_t carries out the differential

mutation to produce the offspring population Q_t. Return to **Step4-3**.

IV. SIMULATION RESULTS

A. SIMULATION PARAMETER SETTING

All of the simulations are completed via the Matlab® platform, version 2014B on a personal computer. The configurations of the computer are CPU 2.80GHz, RAM 16.0GB, and 64-bit operation system. In this paper, the simulation experiment is carried out based on the CyberShip III tug model with a 1:30 reduction ratio. The length, breadth, draft and weight of the ship model are shown in Table 1. The maximum forward thrust, maximum reverse thrust and maximum power of the thrusters are shown in Table 2 [4], [31]. $T_{f\max}$ represents the maximum forward thrust, $T_{f\min}$ represents the maximum reverse thrust, and $P_{\max}$ represents the maximum power. The thruster layout of the simulation ship is shown in Table 3.

TABLE 1. Main dimensions of the Cybership III.

Parameters	1:30 MODEL	Real ship	Unit
Length	1.97	59.1	[m]
Breadth	0.44	13.2	[m]
Draft	0.16	4.8	[m]
Weight	89	2670	[t]

TABLE 2. Parameters of thrusters.

Ship/ model	PROPELLER NUMBER	1#	2#	3#	4#
Real ship	$T_{f\max}$ [KN]	235	365	351	16
	$T_{f\min}$ [KN]	-127	-273	-243	-13
	$P_{\max}$ [MW]	1.2	2.6	2.4	0.031
1:30 model	$T_{f\max}$ [KN]	8.7	13.5	13	0.85
	$T_{f\min}$ [KN]	-4.7	-10.1	-9	-0.57
	$P_{\max}$ [MW]	30.8	27.2	40.8	6.18

TABLE 3. Layout of ship thrusters.

PROPELLER NUMBER	1#	2#	3#	4#
Coordinate l_x (m)	0.74	-0.81	-0.81	0.84
Coordinate l_y (m)	0.0	-0.11	0.11	0.0

The vessel moves from the initial state [0*m* 0*m* 0°] to the desired position [10*m* 10*m* 30°] and maintains the desired heading as shown in Fig.4. The desired longitudinal thrust, the lateral thrust, and the moment of 200s are shown in Figs.5-7.

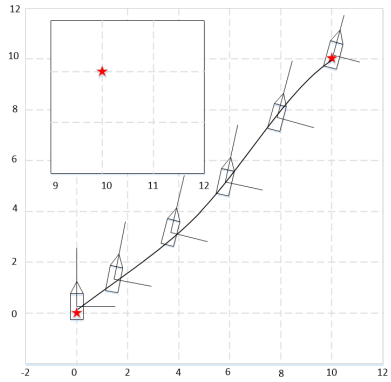

FIGURE 4. Desired ship trajectory.

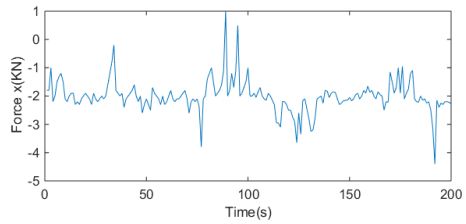

FIGURE 5. Desired longitudinal resultant force.

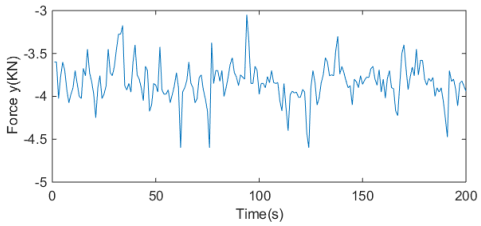

FIGURE 6. Desired lateral resultant force.

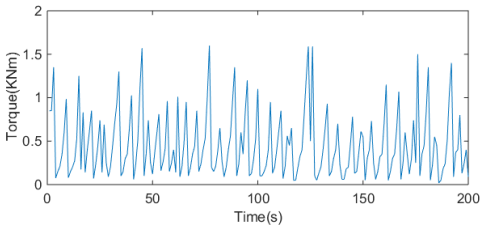

FIGURE 7. Desired moment.

The initial population size is $n = 70$, the number of iterations is $N_{p\max} = 100$, the crossover probability is $P_c = 0.65$. The algorithm has an optimized stall size of $N_{ps} = 10$ and an optimization time limit of $T_{\lim} = 300ms$.

B. RESULTS ANALYSIS

Figs. 8-10 show the angles and thrust states of the three azimuth thrusters during the simulation. The yellow and blue lines represent the results of SQP and INSGA-II, respectively. Fig.11 shows the change in thrust of the tunnel thruster 4#. Since the tunnel thruster is fixed in direction, there is no angular state. It can be seen from the figure that the range and rate of change of the angle and thrust of the thruster under SQP are greater than those of the INSGA-II algorithm. From the

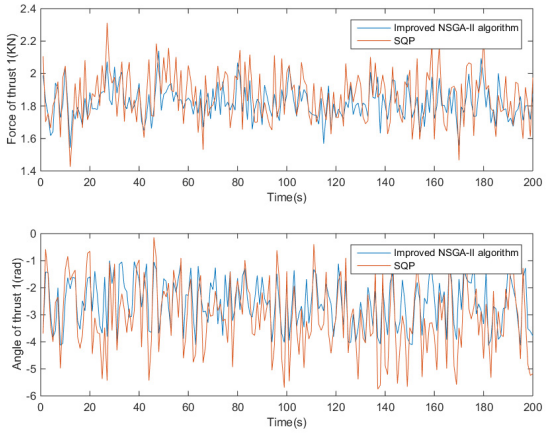

FIGURE 8. Thrust and the angel of thruster #1.

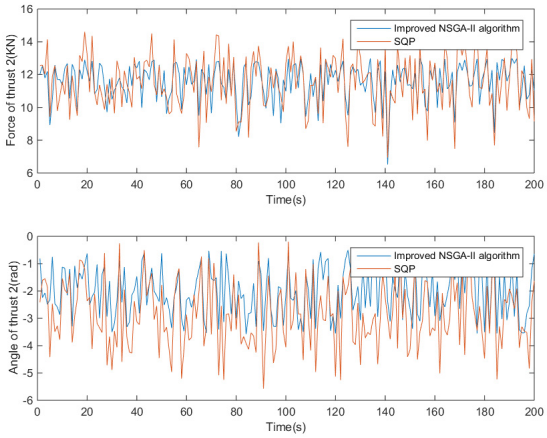

FIGURE 9. Thrust and the angel of thruster #2.

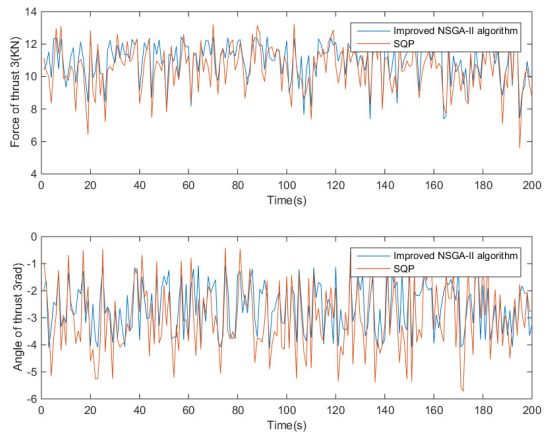

FIGURE 10. Thrust and the angel of thruster #3.

mechanical properties of the propeller, we hope that the propeller will minimize the repeated wear and tear while meeting the desired demand. Obviously, the results of INSGA-II can better meet the requirements of actual working conditions.

According to (6), all thrusters produce a resultant force or moment in surge, sway and yaw. As shown in Figs. 12-14, the yellow and blue lines indicate the results under SQP and NSGA-II, respectively. The resultant

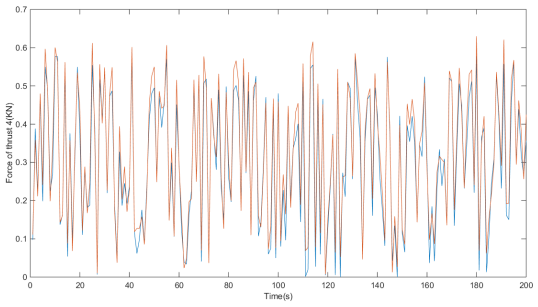

FIGURE 11. Thrust and the angel of thruster #4.

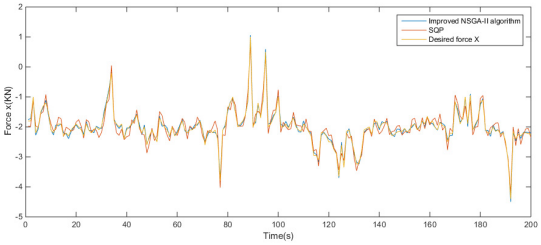

FIGURE 12. Results of longitudinal thrust.

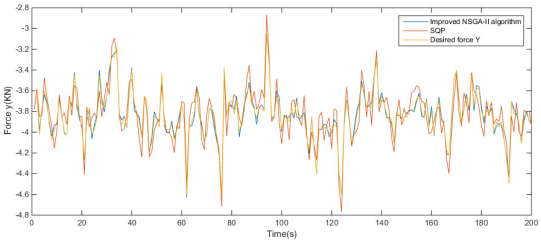

FIGURE 13. Results of lateral thrust.

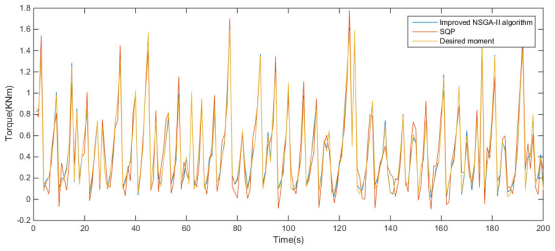

FIGURE 14. Results of moment.

force obtained by the INSGA-II algorithm is very close to the target $\tau_{\mathbf{d}}$. While the SQP algorithm takes more time to reach the expected value when input $\boldsymbol{\tau}_{\mathbf{d}}$ changes. And the maximum error Max and the average error Ave of the SQP algorithm compared to the INSGA-II algorithm are both large. Fig.12 shows the comparison of the results of SQP and INSGA-II with the desired resultant force in surge. Fig.13 shows the comparison of the results of SQP and INSGA-II with the desired resultant force in sway. Fig.14 shows the comparison of the results of SQP and INSGA-II with the desired moment in yaw. Among them, the orange and blue lines indicate the results under SQP and INSGA-II, respectively. The yellow line indicates the set of desired values. Table 4 shows that the average resultant force or moment errors of SQP in

TABLE 4. Tracking errors of the two algorithms.

		X(KN)	Y(KN)	m(KNm)
SQP	Max	0.2992	0.1968	0.1972
	Ave	0.1542	0.0988	0.0967
INSGA-II	Max	0.0987	0.0499	0.0498
	Ave	0.0458	0.0247	0.0218

the direction of surge, sway and yaw are 0.1542 KN, 0.0988 KN and 0.0967 KNm, respectively. The average resultant force or moment errors of INSGA-II in three DOFs are 0.0458 KN, 0.0247 KN and 0.0218 KNm, respectively. The maximum resultant force or moment errors of SQP in three DOFs are 0.2292 KN, 0.1968 KN and 0.1970 KNm, respectively. However, the maximum resultant force or moment errors of the INSGA-II in three DOFs are 0.0987 KN, 0. 0499 KN, and 0. 0498 KNm, respectively. By comparing the results of INSGA-II with those of SQP, the average thrust errors of INSGA-II in surge, sway and yaw are 29.7%, 25% and 22.5% of those of SQP, respectively. This is because the SQP algorithm cannot accurately model the rate at which the thrust magnitude changes. The magnitude of the thrust obtained by the SQP algorithm changes frequently, and the desired force and torque cannot be accurately tracked. The repeated changes in the magnitude of the thrust and the frequent changes in the angle of the propeller cause mechanical wear of the propulsion device and do not conform to its physical conditions. While the INSGA-II algorithm can prevent the azimuth thrust from changing the propulsion angle frequently while satisfying the combined demand.

The orange and blue lines in Fig.15 represent the power consumption of SQP and INSGA-II, respectively. As can be seen from Table 5, the average power consumption under SQP is 37.43W, while the average power consumption under INSGA-II is only 30.09W. The maximum power consumption under SQP is 98.42W, while the maximum power consumption under INSGA-II is 84.65W. The maximum power consumption and average power consumption of INSGA-II are 86.1% and 80.4% of those of SQP, respectively.

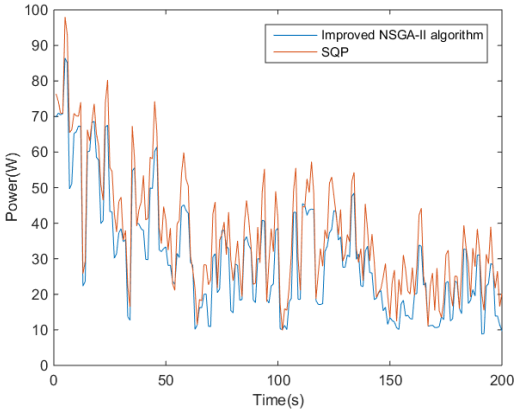

FIGURE 15. Comparison of power consumption.

TABLE 5. Power consumption comparison of the two algorithms.

	$P_{max(w)}$	$P_{min(w)}$	$P_{ave(w)}$
SQP	98.42	9.76	37.43
INSGA-II	84.65	7.61	30.09

Simulation results show that the proposed algorithm has better accuracy and lower average power consumption than the SQP algorithm. In order to achieve the same goals as the INSGA-II algorithm, SQP often needs to allocate a larger output to each thruster, resulting in a higher overall power consumption and peak power, as shown in Table 5. The SQP algorithm is based on the gradient estimation algorithm. When the feasible range of the thrust allocation is large, the local optimal solution may be obtained to meet the thrust demand to a certain extent but the target problem cannot be optimized. The INSGA-II algorithm can achieve higher energy efficiency because it can jump out of the local minimum region and instantly select the global optimal solution for multi-objective problems. It can change the angle of the full-turn propeller to meet the current combined forces and reduce the power consumption.

V. CONCLUSION

This paper proposes a TA method based on the INSGA-II algorithm. In order to improve the problem that the non-dominated individuals with large crowding distance and large solution density are present in the NSGA-II algorithm, the mutation operator in DE is introduced. Simulation results show that the INSGA-II algorithm has less power consumption and error than the SQP algorithm in handling the TA problem, and its computational scale has also been improved. This proves that the proposed strategy is successful and effective. However, the improved NSGA-II algorithm has only been tested with simulated data, and the full-turn propeller is constantly evolving. Therefore, real data should be used for physical testing in the next step, and attempts should be made to introduce more specific operators to achieve better performance for the optimization problem.

REFERENCES

[1] J. F. Hansen and F. Wendt, "History and state of the art in commercial electric ship propulsion, integrated power systems, and future trends," *Proc. IEEE*, vol. 103, no. 12, pp. 2229–2242, Dec. 2015.
[2] P. S. Wang, "Research on hydrodynamic performance of full-revolving propulsions," Ph.D. dissertation, College Shipbuilding Eng., Harbin Eng. Univ., Harbin, China, 2007.
[3] C. O. Lim, B. C. Park, J. C. Lee, E. S. Kim, and S. C. Shin, "Electric power consumption predictive modeling of an electric propulsion ship considering the marine environment," *Int. J. Nav. Archit. Ocean Eng.* vol. 11, no. 2, pp. 765–781, Jul. 2019.
[4] E. Ruth, "Propulsion control and thrust allocation on marine vessels," Ph.D. dissertation, Dept. Mar. Technol., Norwegian Univ. Sci. Technol., Trondheim, Norway, 2008.
[5] T. I. Fossen, *Guidance and Control of Ocean Vehicles*. Hoboken, NJ, USA: Wiley, 1994.
[6] T. I. Fossen and S. I. Sagatun, "Adaptive control of nonlinear systems: A case study of underwater robotic systems," *J. Robotic Syst.*, vol. 8, no. 3, pp. 393–412, Jun. 1991.

[7] T. A. Johansen, T. I. Fossen, and P. Tøndel, "Efficient optimal constrained control allocation via multiparametric programming," *J. Guid., Control, Dyn.*, vol. 28, no. 3, pp. 506–515, 2005.
[8] C. C. Liang and W. H. Cheng, "The optimum control of thruster system for dynamically positioned vessels," *Ocean Eng.*, vol. 31, no. 1, pp. 97–110, Jan. 2004.
[9] Y. Zhang, J. Lu, and H. Tian, "A novel improved adaptive genetic algorithm for the solution to optimal assignment problem," *Int. J. Syst. Control*, vol. 2, no. 3, pp. 253–261, 2007.
[10] D. Karaboga, "An idea based on honey bee swarm for numerical optimization," Dept. Comput. Eng., Fac. Eng., Erciyes Univ., Kayseri, Turkey, Tech. Rep.-tr06, 2005, vol. 200.
[11] D. Fuguang, H. Wei, Z. Lin, and M. Yanqin, "Study on thrust allocation based on IAFSA for dynamic positioning system," in *Proc. 34th Chin. Control Conf. (CCC)*, Jul. 2015, pp. 2362–2366.
[12] P. Yadav, R. Kumar, S. K. Panda, and C. S. Chang, "Optimal thrust allocation for semisubmersible oil rig platforms using improved harmony search algorithm," *IEEE J. Ocean. Eng.*, vol. 39, no. 3, pp. 526–539, Jul. 2014.
[13] G. Q. Xia, C. Y. Liu, X. Y. Chen, and J. Li, "Study on thrust allocation method based on NSGA-II for DP ship," (in Chinese), *J. Huazhong Univ. Sci. Technol.*, vol. 47, no. 5, pp. 101–104, 2019.
[14] D. F. Wu, F. K. Ren, and W. D. Zhang, "An energy optimal thrust allocation method for the marine dynamic positioning system based on adaptive hybrid artificial bee colony algorithm," *Ocean Eng.*, vol. 118, pp. 216–226, May 2016.
[15] L. Zhao and M. I. Roh, "A thrust allocation method for efficient dynamic positioning of a semisubmersible drilling rig based on the hybrid optimization algorithm," *Math. Problems Eng.*, vol. 2015, Aug. 2015, Art. no. 183705.
[16] W. Guo, W. Li, Q. Zhang, L. Wang, Q. Wu, and H. Ren, "Biogeography-based particle swarm optimization with fuzzy elitism and its applications to constrained engineering problems," *Eng. Optim.*, vol. 46, no. 11, pp. 1465–1484, Nov. 2014.
[17] N. T. Dong, "Design of hybrid marine control systems for dynamic positioning," Ph.D. dissertation, Fac. Eng., Nat. Univ. Singapore, Singapore, 2005.
[18] V. Hassani, A. J. Sørensen, and A. M. Pascoal, "A novel methodology for robust dynamic positioning of marine vessels: Theory and experiments," in *Proc. Amer. Control Conf.*, Jun. 2013, pp. 560–565.
[19] B. Ye, J. Xiong, Q. Wang, and Y. Luo, "Design and implementation of pseudo-inverse thrust allocation algorithm for ship dynamic positioning," *IEEE Access*, to be published. doi: 10.1109/ACCESS.2019.2923718.
[20] T. A. Johansen, T. I. Fossen, and S. P. Berge, "Constrained nonlinear control allocation with singularity avoidance using sequential quadratic programming," *IEEE Trans. Control Syst. Technol.*, vol. 12, no. 1, pp. 211–216, Jan. 2004.
[21] A. Ahani and M. J. Ketabdari, "Alternative approach for dynamic-positioning thrust allocation using linear pseudo-inverse model," *Appl. Ocean Res.*, vol. 90, Sep. 2019, Art. no. 101854.
[22] A. Veksler, T. A. Johansen, F. Borrelli, and B. Realfsen, "Cartesian thrust allocation algorithm with variable direction thrusters, turn rate limits and singularity avoidance," in *Proc. IEEE Conf. Control Appl. (CCA)*, Oct. 2014, pp. 917–922.
[23] O. J. Sørdalen, "Optimal thrust allocation for marine vessels," *Control Eng. Pract.*, vol. 5, no. 9, pp. 1223–1231, Sep. 1997.
[24] B. Qi, B. Nener, and X. M. Wang, "An improved NSGA-II based control allocation optimisation for aircraft longitudinal automatic landing system," *Int. J. Control*, vol. 92, no. 4, pp. 705–716, 2019.
[25] B. Qi, B. Nener, and X. M. Wang, "A modified NSGA-II for solving control allocation optimization problem in lateral flight control system for large aircraft," *IEEE Access*, vol. 7, pp. 17696–17704, 2019.
[26] H. F. Wang, "A hybrid evolutionary algorithm with adaptive multi-population strategy for multi-objective optimization problems," *Soft Comput.*, vol. 21, no. 20, pp. 5975–5987, 2017.
[27] Z. B. Zhao, H. R. Liu, B. Liu, and Y. Wen, "Optimization of grate cooler parameters based on improved no-dominated sorting genetic algorithm II," (in Chinese), *Control Decis.*, vol. 8, no. 1, pp. 1–9, 2019.
[28] X. P. Li, G. Dai, M. Wang, Z. Liao, and K. Ma, "A two-stage ensemble of differential evolution variants for numerical optimization," *IEEE Access*, vol. 7, pp. 56504–56519, 2019.
[29] Q. Q. Fan, X. F. Yan, and Y. L. Zhang, "Auto-selection mechanism of differential evolution algorithm variants and its application," *Eur. J. Oper. Res.*, vol. 270, no. 2, pp. 636–653, 2018.
[30] J. Liang, W. Xu, C. Yue, K. Yu, H. Song, O. D. Crisalle, and B. Qu, "Multimodal multiobjective optimization with differential evolution," *Swarm Evol. Comput.*, vol. 44, pp. 1028–1059, Feb. 2019.
[31] Y. Chen, H. Xu, H. Feng, W. Yu, and T. Li, "Adaptive group bias thrust allocation algorithm based on energy optimization," in *Proc. 29th Int. Ocean Polar Eng. Conf. Int. Soc. Offshore Polar Eng.*, Jul. 2019, pp. 171–177.

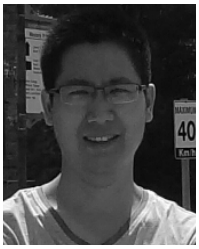

DIJU GAO received the B.E. and M.E. degrees in electrical engineering and automation from Shanghai Maritime University, Shanghai, China, in 2001 and 2008, respectively.

He has been a Teacher with Shanghai Maritime University, since 2001, where he has also been a Senior Engineer with the Key Laboratory of Marine Technology and Control Engineering of Ministry of Transport, since 2014. His research interests include ship electric propulsion systems and hybrid power systems.

XUYANG WANG was born in Fuyang, China, in 1995. He received the bachelor's degree in engineering from Anhui Polytechnic University, Wuhu, China, in 2017. He is currently pursuing the master's degree in electrical engineering with Shanghai Maritime University, China.

His research interests include ship electric propulsion systems and ship automatic control.

TIANZHEN WANG was born in Qingdao, China, in 1978. She received the B.E. and Ph.D. degrees in electrical engineering from Shanghai Maritime University, Shanghai, China, in 2006.

She held a postdoctoral position at the Naval Academy Research Institute of France, Brest, France, from 2007 to 2008. Since 2006, she has been with the Department of Electrical Engineering, Shanghai Maritime University, where she is currently a Professor. Her research interests include fault detection and diagnosis methods, and intelligent information processing.

YIDE WANG received the B.S. degree in electrical engineering from the Beijing University of Post and Telecommunication, Beijing, China, in 1984, and the M.S. and Ph.D. degrees in signal processing and telecommunications from the University of Rennes, France, in 1986 and 1989, respectively. He has authored or coauthored seven chapters in five scientific books, 100 journal articles, and more than 100 national or international conferences. He has also coordinated or managed 15 National or European collaborative research programs. His research interests include array signal processing, spectral analysis, nonlinear control systems, and mobile wireless communication systems.

XIAOBIN XU is currently a Professor with the Department of Automation, Hangzhou Dianzi University, and the Belt and Road Information Technology Research Institute. His research interests include fuzzy set theory, evidence theory and its applications in the processing of uncertain information, the reliability analysis, safety evaluation, and condition monitoring of complex industrial systems.